Copyright © 2010 American Scientific Publishers
All rights reserved
Printed in the United States of America

Journal of
Nanoscience and Nanotechnology
Vol. 10, 4240–4245, 2010

Compression Behaviour of Thick Vertically Aligned Carbon Nanotube Blocks

Matteo Pavese[1], Simone Musso[2,*], and Nicola M. Pugno[3]

[1] *Dipartimento di Scienza dei Materiali e Ingegneria Chimica, Politecnico di Torino, Corso Duca degli Abruzzi 24, 10129 Torino, Italy*
[2] *Dipartimento di Fisica, Politecnico di Torino, Corso Duca degli Abruzzi 24, 10129 Torino, Italy*
[3] *Dipartimento di Ingegneria Strutturale e Geotecnica, Politecnico di Torino, Corso Duca degli Abruzzi 24, 10129 Torino, Italy*

Blocks of vertically aligned multiwall carbon nanotubes were prepared by thermal chemical vapor deposition starting from camphor and ferrocene precursors. The blocks, having a thickness of approximately 2 mm and composed of nanotubes with diameter ranging between 30 and 80 nm, were submitted to compression tests. The results were analyzed accordingly with a simple model consisting in a parallel array of nanotubes under compression and bending suffering microscopic instability and compaction. The model mostly fits the experimental stress-strain curves, with a small deviation attributed to dissipative phenomena, such as frictional forces and nanotube wall breakage.

Delivered by Ingenta to:
Rice University, Fondren Library
IP: 168.7.12.7
Sat, 17 Jul 2010 14:26:58

Keywords: Aligned CNTs, CVD, Mechanical Properties, Nano Tube Devices.

1. INTRODUCTION

Blocks of vertically aligned (VA) carbon nanotubes (CNTs) can be produced mainly by gas-phase (or vapour-phase) techniques, classified as thermal chemical vapour deposition (CVD)[1,2] and plasma enhanced CVD (PE-CVD),[3] accordingly to the energy source used to provoke the carbon precursor cracking. In particular, for its low cost, simplicity and versatility, thermal CVD method offers the best path toward large scale production.[4]

The synthesis of large blocks of millimetre long VACNTs would ideally allow to transfer to a macroscopic level the impressive chemical/physical properties of carbon nanotubes (both single and multi walled),[5,6] enabling the scientific world to produce a new class of anisotropic materials which are very interesting due to their potential application in several areas such as heat sinks for high power electronic devices,[7] strong adhesive materials,[8,9] membranes and filters,[10] reinforcement for composite materials[11] and so on. In the field of reinforcement for composite materials, polymeric films reinforced with aligned CNTs have been studied[12] as possible candidates for mechanical damping applications due to the energy dissipation caused by nanotube-polymer interfacial shear friction.

However, it is interesting to notice that while not perfectly stretched and aligned CNTs can suffer a significant reduction in mechanical properties at microscopic level due to the lattice defectiveness[13] (e.g., an isolated CNT with a single vacancy can suffer a 20% strength reduction),[14,15] the overall toughness of a large block can be enhanced. In fact, under compressive stress, the entangled structure of the nanotubes can produce a great amount of friction and energy dissipation.[11,16]

In this work we performed compressive loading tests on self-standing millimetre thick blocks of as-grown multiwall (MW) carbon nanotubes with a significant entanglement degree among contiguous nanotubes. The CNT carpet, deposited on bare silicon wafers by CVD from camphor and ferrocene, exhibited a density of approximately 0.1–0.3 g/cm^3. The observed stress–strain curves revealed an elastic–plastic–hyperelastic compressive behaviour. The experimental evidences were consistent with a simple mechanical model consisting in a parallel array of nanotubes under compression and bending, that develops microscopic instability and compaction. Deviations of the experimental curves from the model were attributed mainly to frictional interaction between nanotubes and their fracture.

2. EXPERIMENTAL DETAILS

Thick layers of VAMWCNTs were prepared by thermal CVD on silicon substrates (100).[17,18] A solid mixture, made with 60 g of commercial camphor and 3 g of ferrocene (98% purity in weight, Aldrich), was heated to its boiling point (around 220 °C) and the so produced vapor

*Author to whom correspondence should be addressed.

 1533-4880/2010/10/4240/006 doi:10.1166/jnn.2010.2187

was carried by a nitrogen gas flow inside the CVD reactor. The reactor consists in a quartz tube (4 cm in diameter) housed in a cylindrical oven. At 850 °C the thermal cracking of the molecules produces reactive carbon species and iron nanoparticles that, depositing on the bare silicon substrate, generate VAMWCNTs by a combination of tip and base growth mechanism.[19, 20] The morphology of the MWCNT's blocks, mechanically delaminated from the substrates by a razor blade, was examined by field emission (FE) scanning electron microscopy (SEM).

Compression tests were performed along the growing direction of the nanotubes by using a Sintech 10D equipment, stroke control with crosshead speed of 0.5 mm/min. Two types of experiments were realized: load tests up to a fixed load (maximum load 44500 N), and load-unload cycles up to a fixed percentage of the sample initial height. After crash loading, FESEM analyses were performed on resulting powder and residual blocks.

Delivered by Ingenta to:
Rice University, Fondren Library
IP : 168.7.127.7
Sat, 17 Jul 2010 14:26:58

3. THEORETICAL

We model the nanotube carpet as inclined, by an angle ϑ (with respect to the vertical axis), identical cantilever beams (see Fig. 1), having cross-sectional area A, moment of inertia I, elastic modulus E, length L and nominal area fraction φ.

During compression between two parallel (horizontal) plates with a nominal stress σ, a (vertical) force $F = \sigma A/\sigma A(\varphi\cos\vartheta)$ is carried by each individual nanotube, resulting in both axial ($N = F\cos\vartheta$) and shear ($T = F\sin\vartheta$) loads and thus resulting in both axial ($u = NL/(EA)$) and transversal ($v = TL^3/(3EI)$) displacements; the nominal strain $\varepsilon = (u\cos\vartheta + v\sin\vartheta)/(L\cos\vartheta)$ is thus related to the nominal stress via the following law:

$$\sigma = E'\varepsilon, \quad E' = \frac{E\varphi}{1+\tan^2\vartheta\lambda^2/3}$$
$$\lambda = L/\rho, \quad \rho = \sqrt{I/A} \qquad (1)$$

describing a linear elastic regime, where ρ is the radius of inertia of the nanotube, λ is its slenderness and E' is the effective elastic modulus of the carpet.

Equation (1) is expected always in tension but in compression only up to reaching the elastic instability of the nanotube, arising when the axial load N equals the Euler load $N_C = \pi EI/(4L^2)$; this happens when the nominal stress reaches:

$$\sigma_P = \frac{\pi E\varphi}{4\lambda^2} \qquad (2)$$

at a strain $\varepsilon_P = \sigma_P/E'$; note that since the Euler load remains constant around the instability configuration the nominal stress σ should not significantly change in the strain range $\varepsilon_P < \varepsilon < \varepsilon'_C$, where ε'_C denotes the strain at which a different mechanism will become significant; thus, for $\varepsilon_P < \varepsilon < \varepsilon'_C$ a macroscopic plastic behaviour is expected, as a consequence of the microscopic elastic instability.

The mentioned additional mechanism is compaction. The full compaction, due to nanotube fracture (and plasticity), is expected with a slope $E' \approx E$ (thus nearly vertical, if compared with the other parts of the curve), at a critical strain $\varepsilon'_C \approx 1 - \varphi S_{in}/S_{fin}$, where $S_{in,\,fin}$ are the areas of the resistant surfaces at the initial and final stages of the test ($S_{in}/S_{fin} < 1$ due to material expulsion). Thus a macroscopic hyperelastic (with very steep stress–strain) regime is expected as a consequence of the microscopic compaction. In Figure 2 a scheme of the expected stress–strain curve is depicted.

In this figure the possibility of fracture and friction of nanotubes before compaction is also considered; fracture would bring to a slightly decrement of the slope in the stress–strain curve, whereas contact and friction between nanotubes would imply a larger stiffness.

To check the contact hypothesis let us assume two different limiting contact configurations, at "X" or "I", corresponding to when the contact between contiguous nanotubes occurs only in the central point ("X", $\alpha = 2$) or on the whole side ("I", $\alpha = 1$) of two adjacent nanotubes

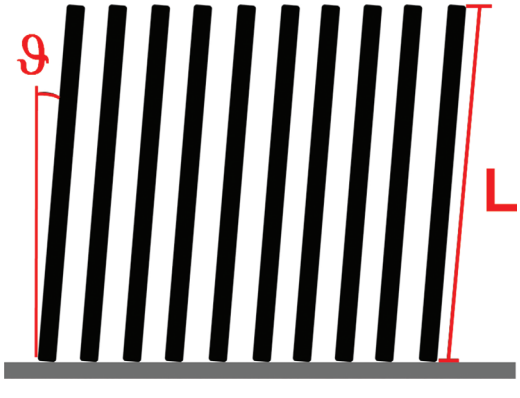

Fig. 1. Scheme of the carbon nanotube block considered in the theoretical model.

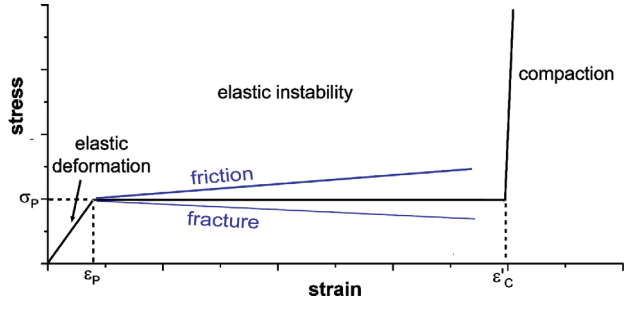

Fig. 2. Theoretical prediction of the mechanical behaviour of CNTs blocks. The friction and fracture phenomena can alter the slope of the curve. Fracture is necessarily expected at compaction, whereas contact and friction is observed from the very beginning.

respectively. Geometrically, we expect their activations at strains ε_C given by:

$$\varepsilon_C \approx \frac{(D/L)^\alpha}{\alpha}, \quad D = \left(\sqrt{\varphi_{\max}/\varphi} - 1\right)R \qquad (3)$$

where D is the distance between two adjacent nanotubes, R is their external radius and $\varphi_{\max}$ is the maximal area fraction (packing factor).

Note that inserting plausible values for our produced VAMWCNTs into Eqs. (1)–(3) (see next Section) suggests $\varepsilon_C < \varepsilon_P < \varepsilon_C^{/}$, thus we expect contact and friction from the very beginning, elastic instability and finally compaction and fracture.

4. RESULTS AND DISCUSSION

Two types of carbon nanotubes blocks were tested in compression. The two materials present a density of 0.12 g/cm^3 and 0.31 g/cm^3 respectively. By comparing the experimental density with the theoretical value of 2.3–2.6 g/cm^3 for MWCNTs[5] it is possible to calculate the fraction of empty volume in the blocks, that is 95% and 86% respectively. The low density of the samples can be confirmed by means of the FESEM images reported in Figure 3. Whereas at lower magnification the samples exhibit a macroscopic alignment, at higher magnification it is possible to appreciate both a significant degree of entanglement among adjacent nanotubes and the empty space around each of them. Moreover, with SEM images we estimated that the sample with lower density (labeled LD from now on for brevity purposes) has MWCNTs with diameters ranging between 35 and 65 nm, while the sample with higher density (labeled HD from now on for brevity purposes) has MWCNTs with diameters ranging between 50 and 80 nm.

During compression tests the resistant surface of the samples grows, since fragments of the nanotubes block are

Delivered by Ingenta to:
Rice University, Fondren Library

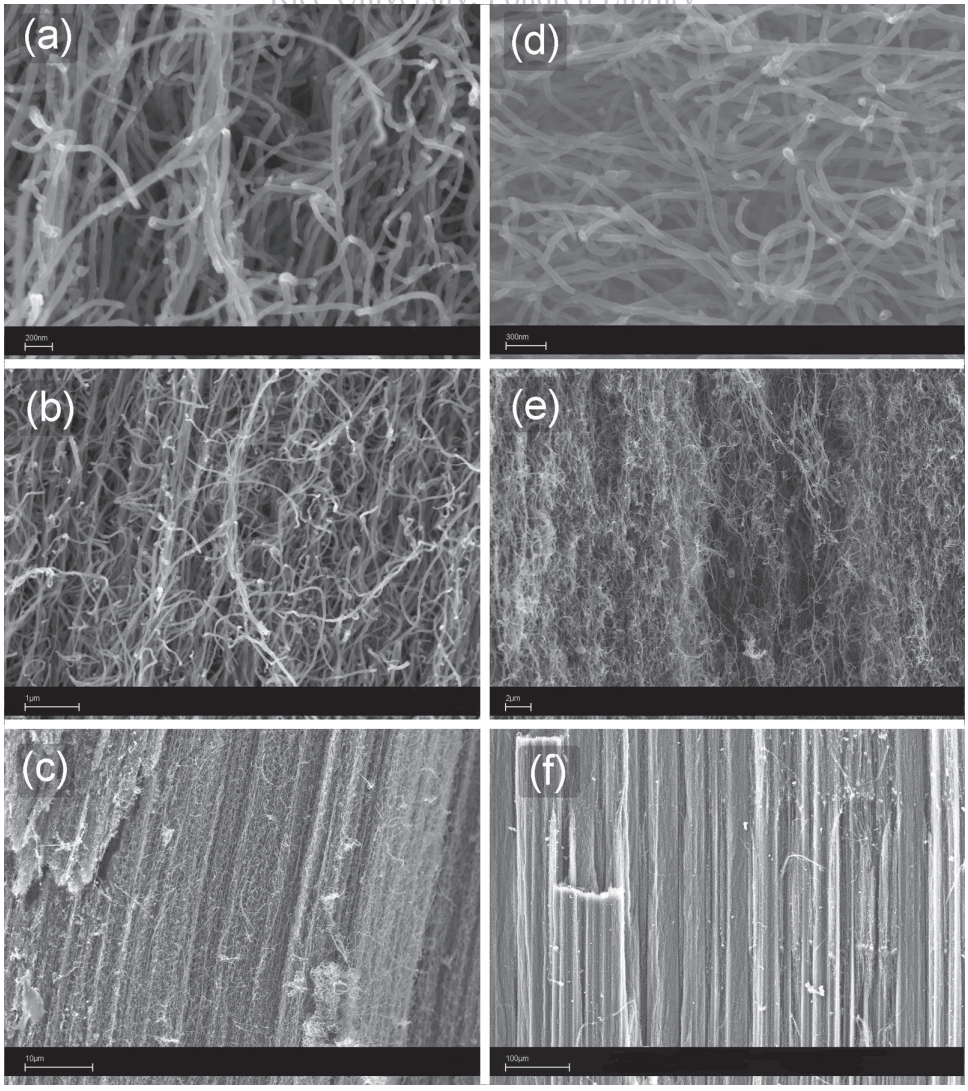

Fig. 3. Side views SEM images of HD (a, b, c) and LD (d, e, f) carbon nanotubes blocks.

pushed on the side of the sample itself. It was verified that the resistant surface at the end of the stress–strain test was roughly double than the initial one, i.e., $S_{in} / S_{fin} \approx 0.5$. Thus it is possible to calculate the expected full compaction strain ($\varphi_{HD} = 0.14$ for HD blocks and $\varphi_{LD} = 0.05$ for LD ones), being $\varepsilon_C^{/HD} = 0.93$ for HD blocks and $\varepsilon_C^{/LD} = 0.98$ for LD ones. From the density and size values it is also possible to calculate the mean distance between two contiguous nanotubes, following Eq. (3) with $\varphi_{max} = 0.9$ (cylinder packing factor) and taking R as the reported mean values, the (mean) CNT distance results to be 50 nm for HD blocks and 80 nm for LD.

In Figure 4 are presented two compression curves, for a typical HD and for a typical LD nanotubes block. It is interesting to note that LD blocks do not present significant mechanical properties in the first part of the curve ($\sigma < 2$ MPa), suggesting a very low Young's modulus (lower than 10 MPa). HD blocks on the contrary shows a Young's modulus around 0.5 GPa in the very first part of the curve and a plateau at a stress ranging from 16 to 36 MPa. The central part of the stress-strain curve for HD blocks presents a complex behaviour. While roughly the stiffness can be considered as zero in this central part, we observe both positive and negative stiffness zones, suggesting both friction and fracture. The last part of the stress-strain curve presents an evident compaction phenomenon, with a rapid increase of Young's modulus and stress. The mean final strain, $\varepsilon_C^{/}$, has a value comparable to the theoretical one, being $\varepsilon_C^{/} \sim 0.94$ for HD blocks and $\varepsilon_C^{/} \sim 0.97$ for LD blocks. The model proposes a good fit of the curve for HD blocks: a first part with the bending of carbon nanotubes followed by the elastic instability zone, where the stiffness is roughly zero. As expected, in the central zone we observe in the experimental stress-strain curve two opposite behaviours: the stress values can locally increase (positive stiffness) or decrease (negative stiffness). This confirms that the hypotheses of friction between contiguous nanotubes (positive stiffness) or fracture of nanotubes (negative stiffness). The proposed model does envisage these phenomena, even if the fine fitting of the curve is out of the scope of the present paper. The stress-strain curve can be considered as roughly flat in the zone from 0.1 to 0.7 strain. The observed small positive slope agrees with the prediction of our model, $\varepsilon_C < \varepsilon_P < \varepsilon_C^{/}$, suggesting the nearly immediate activation of the contact and friction between nanotubes. In particular, in the model we predicted ε_C in two configurations (I and X), hypothesising that the contact between contiguous nanotubes occurs on the whole side of the nanotubes or only in the central point. For both I and X cases, the value of ε_C can be calculated from experimental data, and it is very low, being around 2–3% strain for I case and lower than 0.01% strain for X case. This confirms that friction occurs from the very beginning of the stress-strain curve. This behaviour is reasonable, since the nanotubes are very long, so that they come in contact one with another at a very low bending strain.

Delivered by Ingenta to:
Duke University, Fondren Library
IP: 128.7.127.7
Sat, 17 Jul 2010 14:36:58

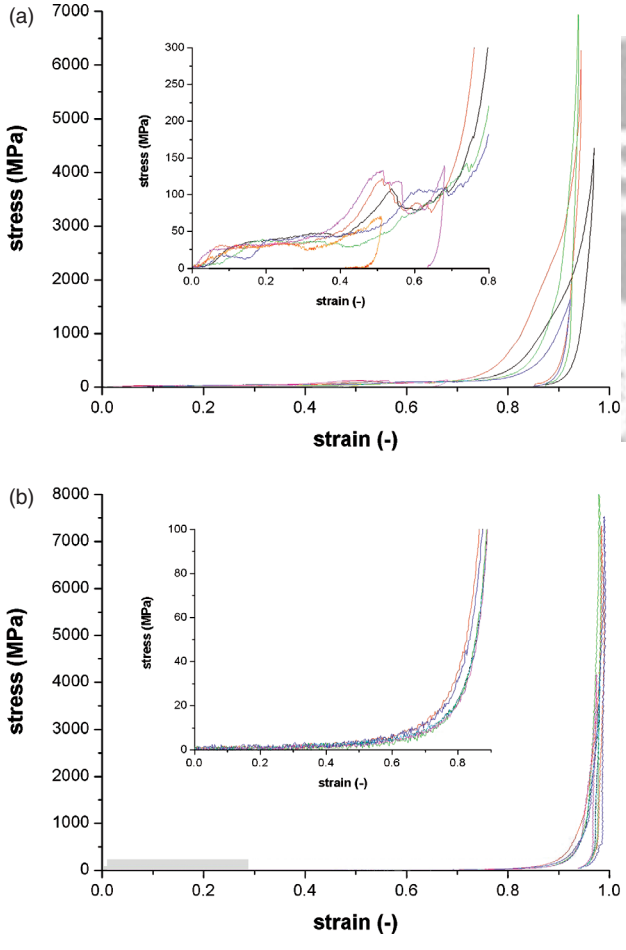

Fig. 4. Compression load/unload curves for a HD block (a) and for a LD block (b). In the inset it is shown a magnification of the low stress zone of the curves.

In Figure 5 SEM images of the nanotubes blocks after compression are reported. Figures 5(a–c) show the HD block after 4 GPa maximum compression. It is evident that the HD block partially maintains its structure even after a high compression load. However cracks are observed throughout the whole surface and section of the block, and the individual carbon nanotubes are fractured. In Figures 5(d–f) a LD block after 3 GPa maximum compression is reported instead. In this case the block loses its shape completely after the compression test, and the nanotubes are broken into short fragments.

In Table I experimental and theoretical results are presented. In order to perform the calculation, the Young's modulus of the nanotubes has been assumed as 500 GPa. The calculation is based on the individuation of E' and σ_P from the stress–strain curve. By fitting the curve with the model it is possible to calculate L and ϑ. The calculated L values are quite low, considering that the CNTs block is

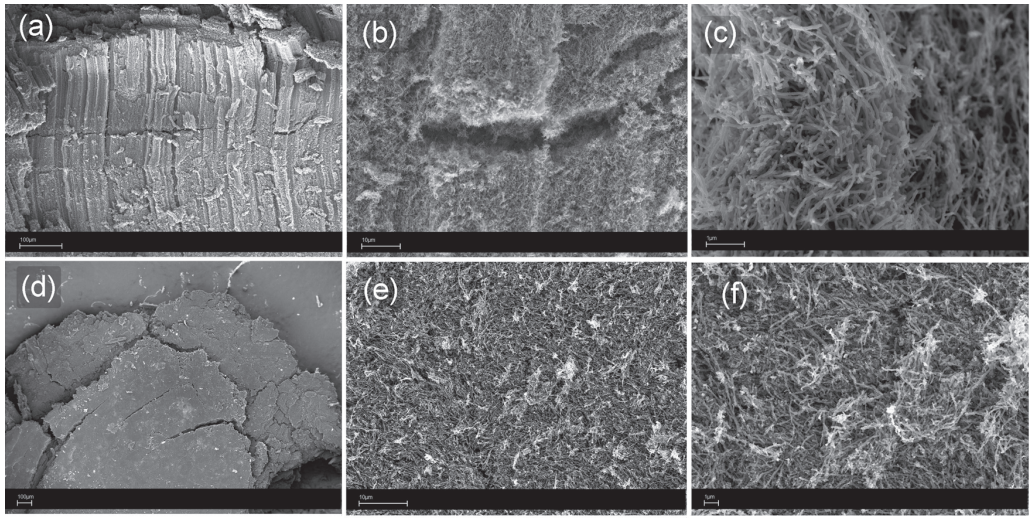

Fig. 5. Side and frontal views SEM images of HD (a, b, c) and LD (d, e, f) carbon nanotube blocks after compression test.

Delivered by Ingenta to:
Rice University, Fondren Library
IP: 168.7.127.7
Sat, 17 Jul 2010 14:26:58

in the millimetric range. However it must be stressed that from the very beginning of the curve friction and possibly fracture can occur, so that L value must be considered not as the real length of the nanotube but as the "free" length of a single nanotube. This result suggests that the mean distance between two contact points between individual nanotubes is in the order of the micrometer. The value is slightly higher for LD blocks, since these blocks are less dense, and consequently the mean free length of the nanotubes is higher. Moreover from ϑ values the model is able to calculate how much the nanotubes are misaligned with respect to the vertical direction. Table I suggests that denser CNTs blocks present a higher orientation degree than lighter ones.

Table I. Experimental and calculated values for HD and LD blocks. The values of the mean free contact distance L and orientation ϑ are calculated to exactly fit the observed values of the fictitious Young's modulus E' and yield stress σ_P. The calculated mean distance between nanotubes are 50 nm for HD and 80 nm for LD blocks, compatible with SEM observations. The contact values of ε_C are lower than 0.01% for initial contact (X geometry) and around 2–3% for the final contact (I geometry), confirming (as experimentally observed from the slightly positive slope of the nearly flat stress–strain region) that friction occurs from the very beginning of the stress–strain curve. The calculated full compaction strains are $\varepsilon_C^{/\mathrm{HD}} = 0.93$ and $\varepsilon_C^{/\mathrm{LD}} = 0.97$, in close agreement with the observed values.

	Experimental		Calculated		
CNT block	E' (GPa)	ε_C'	σ_C (MPa)	L (μm)	ϑ (deg)
HD1	0.54	0.92	20	1.8	12
HD2	0.74	0.94	31	1.5	12
HD3	0.55	0.97	27	1.6	13
HD4	0.33	0.94	36	1.4	20
HD5	0.62	—	24	1.7	12
HD6	0.46	—	16	2.1	11
HD (mean value)	0.54	0.94	26	1.7	13
LD (any block)	<0.01	0.98	<2	>2.5	>26

5. CONCLUSIONS

Blocks of vertically aligned multiwalled carbon nanotubes have been prepared by thermal CVD and tested under compression. The results have been rationalized according to an elastic model suggesting the occurrences of different phenomena, such as contact and friction between nanotubes, their elastic instability and finally their compaction and fracture. In particular, the contact initiates at the very beginning, for strains lower than 0.01% and is fully established at strains of ~3%. At a strain of ~4% the elastic instability begins (under a nominal stress of several megapascals). The full compaction is observed for strains of ~95%. These complex and dissipative mechanisms, that could be tailored with our CVD process and theoretical model, suggest that VACNTs could be of great interest for high-nanotech applications as shock-absorbers.

References and Notes

1. X. Zhang, A. Cao, B. Wie, Y. Li, J. Wie, C. Xu, and D. Wu, *Chem. Phys. Lett.* 362, 285 **(2002)**.
2. X. Li, A. Cao, Y. Joon Jung, R. Vajtai, and P. M. Ajayan, *Nanoletters* 5, 1997 **(2005)**.
3. M. Chhowalla, K. B. K. Teo, C. Ducati, N. L. Rupesinghe, G. A. J. Amaratunga, A. C. Ferrari, D. Roy, J. Robertson, and W. I. Milne, *J. Appl. Phys.* 90, 5308 **(2001)**.
4. C. Oncel and Y.Yurum, Fullerenes, Nanotubes, and Carbon Nanostructures **(2006)**, Vol. 14, p. 17.
5. H. J. Qi, K. B. K. Teo, K. K. S. Lau, M. C. Boyce, W. I. Milne, J. Robertson, and K. K. Gleason, *J. Mech. Phys. Solids.* 51, 2213 **(2003)**.
6. T. Borca-Tasciuc, M. Mazumder, Y. Son, S. K. Pal, L. S. Schdler, and P. M. Ajayan, *J. Nanosci. Nanotechnol.* 7, 1581 **(2007)**.
7. K. Kordás, G. Tóth, P. Moilanen, M. Kumpumäki, J. Vähäkangas, A. Uusimäki, R. Vajtai, and P. M. Ajayan, *Appl. Phys. Lett.* 90, 123105 **(2007)**.
8. L. Qu, L. Dai, M. Stone, Z. Xia, and Z. L. Wang, *Science* 322, 238 **(2008)**.

9. N. Pugno, *J. Phys. Cond. Mat.* 19, 395001 **(2007)**.
10. A. Srivastava, O. N. Srivastava, S. Talapatra, R. Vajtai, and P. M. Ajayan, *Nature Materials* 3, 610 **(2004)**.
11. J. Suhr, P. Victor, L. Ci, S. Sreekala, X. Zhang, O. Nalamasu, and P. M. Ajayan, *Nature Nanotechnology* 2, 417 **(2007)**.
12. N. Koratkar, B. Q. Wei, and P. M. Ajayan, *Adv. Mater.* 14, 997 **(2002)**.
13. N. Pugno, *Appl. Phys. Lett.* 90, 043106 **(2007)**.
14. N. Pugno and R. Ruoff, *Philos. Mag.* 84, 2829 **(2004)**.
15. N. Pugno, *Int. J. Fract.* 140, 159 **(2006)**.
16. E. H. T. Teo, W. K. P. Yung, D. H. C. Chua, and B. K. Tay, *Adv. Mater.* 19, 2941 **(2007)**.
17. M. Kumar and Y. Ando, *Chem. Phys. Lett.* 374, 521 **(2003)**.
18. S. Musso, S. Porro, M. Giorcelli, A. Chiodoni, C. Ricciardi, and A. Tagliaferro, *Carbon* 45, 1133 **(2007)**.
19. L. M. D. Dell'Acqua-Bellavitis, J. D. Ballard, P. M. Ajayan, and R. W. Siegel, *Nano Lett.* 4, 1613 **(2004)**.
20. M. Pinault, V. Pichot, H. Khodja, P. Launois, C. Reynaud, and M. M. L'Hermite, *Nano Lett.* 5, 2394 **(2005)**.

Received: 30 April 2009. Accepted: 30 June 2009.

Delivered by Ingenta to:
Rice University, Fondren Library
IP : 168.7.127.7
Sat, 17 Jul 2010 14:26:58